Inelastic-neutron-scattering studies of poly(*p*-phenylene vinylene)

P. Papanek
Department of Materials Science and Engineering and Laboratory for Research on the Structure of Matter, University of Pennsylvania, Philadelphia, Pennsylvania 19104

J. E. Fischer
Department of Materials Science and Engineering and Laboratory for Research on the Structure of Matter, University of Pennsylvania, Philadelphia, Pennsylvania 19104
and Materials Science and Engineering Laboratory, National Institute of Standards and Technology, Gaithersburg, Maryland 20899

J. L. Sauvajol
Groupe de Dynamique des Phases Condensées, Université Montpellier II, Montpellier Cedex 05, France

A. J. Dianoux
Institut Laue-Langevin, 38042 Grenoble Cedex, France

G. Mao and M. J. Winokur
Department of Physics, University of Wisconsin, Madison, Wisconsin 53706

F. E. Karasz
Department of Polymer Science and Engineering, University of Massachusetts, Amherst, Massachusetts 01003
(Received 3 March 1994; revised manuscript received 7 July 1994)

Mode polarization and energy spectra for the lattice modes of poly(*p*-phenylene vinylene) are obtained by inelastic-incoherent-neutron-scattering methods. Experiments were performed on stretch-oriented, highly crystalline films with time-of-flight and filter-analyzer spectrometers. By measuring all-hydrogen and vinylene-deuterated samples, we show that almost all of the observed modes can be attributed to phenylene motions. The low-energy features in the vibrational density of states consist of a longitudinal 2.5-meV mode assigned to a damped translational motion along the chain axis, a 7-meV phenyl ring in-phase librational mode (transverse with respect to the chain axis), and strong bands at 15 and 25 meV showing mixed polarization, the latter also displaying negative frequency shift with increasing temperature. Higher-frequency modes are in excellent agreement with published infrared and Raman studies, as well as with the results of our vibrational analysis based on the semiempirical AM1 method.

I. INTRODUCTION

Poly(*p*-phenylene vinylene) (PPV) is a prototypical conjugated polymer with a nondegenerate ground state. The polymer chains are composed of alternating phenylene rings (–C_6H_4–) and vinylene segments (–CH=CH–) as shown in Fig. 1(a). PPV exhibits interesting electronic[1] and nonlinear optical properties,[2] and the electrical conductivity of a highly stretched film of PPV after doping with concentrated sulfuric acid is reported to be as high as 1.12×10^4 S cm^{-1}.[3] PPV derivatives can be used to fabricate light-emitting diodes.[4]

PPV films synthesized by thermal conversion and simultaneous uniaxial stretching of soluble precursors exhibit a high degree of crystallinity and relatively large coherence lengths.[5] Several electron and x-ray diffraction measurements have been performed in order to determine the crystal structure, yielding similar results.[5–8] The interchain packing is very regular, with the characteristic herringbone arrangement of two inequivalent chains per projected two-dimensional rectangular unit cell ($p2gg$ symmetry), Fig. 1(b). The Bravais lattice is monoclinic with nominal parameters $a = 8.0$ Å, $b = 6.0$ Å, c (along the chain axis) $= 6.6$ Å, the monoclinic angle $\alpha = 123°$, and the chain setting angle (with respect to the a axis) is about 52°.

Improved refinements of the equatorial structure were achieved in a recent x-ray diffraction study of highly oriented PPV.[9] These suggested a nonplanar thermal-average chain conformation as well as large-amplitude phenylene ring librations. The value of the *average* dihedral angle ϑ_D formed by the plane of the phenylene ring and that of the vinylene segment, as well as the librational displacement about that average ϑ_L, were found to increase with temperature: from $\vartheta_D = 8°$ and $\vartheta_L = 9°$ at 293 K to $\vartheta_D = 13°$ and $\vartheta_L = 18°$ at 673 K. Significant librational and ring-flip (180° rotational jump) motions have also been identified in NMR studies of partially labeled PPV,[10] and the nonplanarity and thermally driven increase of ϑ_D and ϑ_L have also been derived from neu-

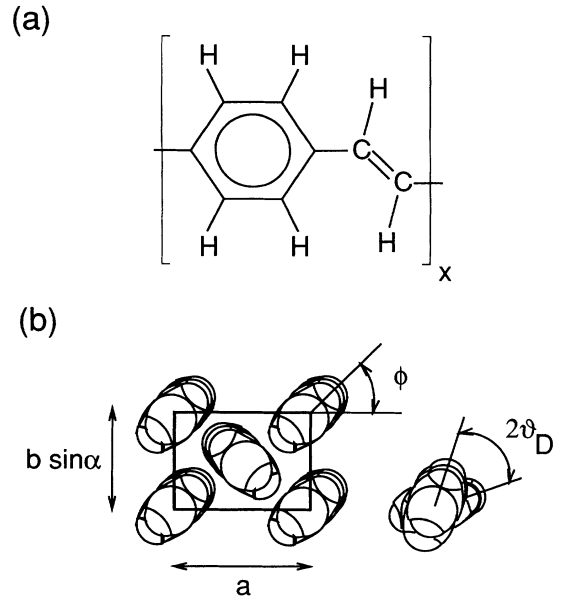

FIG. 1. (a) The chemical structure of poly(*p*-phenylene vinylene). In the partially deuterated sample the hydrogens of the vinylene segments (–CH=CH–) are replaced by deuterium. (b) The typical herringbone packing of PPV chains viewed along the *c* axis. The chain setting angle ϕ and the dihedral angle ϑ_D are also illustrated.

tron diffraction experiments on all-hydrogen and selectively deuterated PPV films.[11]

Diffusion of dopant ions provokes substantial changes in the host structure, which can be generally described in terms of single-chain rotations and translations.[12] Furthermore, the intrachain vibrations (particularly those of the phenylene rings) and the concomitant changes in dihedral angle are believed to be closely related to the electronic properties of the polymer.[13] Therefore, detailed knowledge of the dynamics is clearly needed. Intrachain vibrational data are available from infrared- and Raman-active modes above 400 cm^{-1} (50 meV), while very little is known about the inter- or intrachain dynamics at lower energies.

In this paper we present the results of incoherent-inelastic-neutron-scattering (IINS) experiments performed on highly oriented PPV films at different temperatures. By this method we have obtained new quantitative information about the lattice and molecular dynamics in the 0–80 meV range. Three approaches have been taken to aid in the assignment of peaks in the scattering function to specific modes: (1) polarization analysis as described in our previous work on polyacetylene[14,15] and polyaniline,[16] (2) selective deuteration which effectively "turns off" the deuterated site to incoherent scattering spectra, and (3) molecular mechanics calculations of single PPV chains at the Austin model 1 (AM1) level.

II. EXPERIMENTAL PROCEDURES AND DATA ANALYSIS

Two complementary scattering techniques, the cold neutron time-of-flight (TOF) method and filter-analyzer spectrometry (FAS), were employed. The former was done on the MIBEMOL instrument at the Laboratoire Léon Brillouin in Saclay, while FAS was performed on the BT4 spectrometer at the NIST reactor. Because in the FAS method the wave-vector transfer $\mathbf{Q} = \mathbf{k}_f - \mathbf{k}_i$ and the energy exchange $\hbar\omega$ are directly related, the excitations are in principle measured over a slice through $(\mathbf{Q}, \omega)$ phase space. On the other hand the TOF instrument can explore larger regions of phase space since the scattered neutrons are collected by many detectors at different angles and over a wide range of final energies. Both methods are described in more detail below.

PPV films were prepared by thermal conversion of stretched precursors as described elsewhere,[17,18] and subsequently annealed under dynamic vacuum at 380 °C for 2.5 h. For the TOF experiments, ~ 250 mg of all-hydrogen film $(C_8H_6)_x$ was folded and wrapped around a thin aluminum plate to form a 2 cm square packet ~ 0.6 mm thick which we estimated to be a 10% scatterer (thus minimizing multiple scattering). The packet was hermetically sealed in a square Al container with the chain axis parallel to a side of the square. For the FAS experiments, the mass of the all-hydrogen sample was increased to 720 mg. We also measured with the FAS technique about 1050 mg of a partially deuterated sample $(C_6H_4C_2D_2)_x$, in which ~ 70% of the vinylene hydrogens were replaced by deuterium. Since the incoherent cross section $\sigma_{inc}(D) = 2.04$ b is much smaller than $\sigma_{inc}(H) = 79.91$ b, the response of this sample reveals almost exclusively the phenylene ring motions. The larger sample mass in FAS was mostly accommodated by a larger area, rectangular rather than square, and so the thickness was still sufficiently small to minimize multiple scattering. The *c*-axis mosaic of both films was determined by x-ray and neutron diffraction to be about 10° [full width at half maximum (FWHM)].

The feasibility of using the TOF method to obtain both polarization and energy information about the lattice modes was demonstrated in previous papers on stretch-oriented *cis*- and *trans*-polyacetylene.[14,15] It was shown that it is possible to discriminate between modes polarized parallel and perpendicular to the chain axis (the *c* axis).

Because hydrogen is a strong incoherent scatterer with a cross section much greater compared to carbon [$\sigma_{coh}(C) = 5.5$ b and $\sigma_{inc}(C) = 0.01$ b], the inelastic scattering is almost exclusively incoherent and sensitive only to hydrogen motions. Furthermore, the scattering function $S_{inc}(\mathbf{Q}, \omega)$ depends on the product $\mathbf{Q} \cdot \mathbf{e}_j^d(\mathbf{q})$, where $\mathbf{e}_j^d(\mathbf{q})$ is the displacement vector of the dth hydrogen atom corresponding to the normal mode j and a phonon wave vector $\mathbf{q}$ in the first Brillouin zone. In the experiment two different scattering geometries, called in the following $C_\perp$ and $C_\parallel$, are designed in such a way that $\mathbf{Q}$ is either predominantly perpendicular or parallel to the chain axis (the *c* axis) of the stretch-oriented polymer, respectively. Thus it is possible to discriminate between vibrational modes with transverse polarization from those polarized along the chains. The experimental setup for this measurement is discussed in more detail in Ref. 14.

In the incoherent approximation $S_{inc}(\mathbf{Q}, \omega)$ is related

to the generalized density of vibrational states $G(\omega)$:[19]

$$S_{\text{inc}}(\alpha,\beta) = \exp[-2W(Q)]\ \frac{\alpha \exp(-\beta/2)}{2\beta \sinh(\beta/2)}\ G(\omega), \quad (1)$$

where $\alpha = \hbar^2 Q^2/(2mk_BT)$, $\beta = \hbar\omega/(k_BT)$, m is the mass of hydrogen, T the temperature, k_B the Boltzmann constant, and $W(Q)$ the Debye-Waller factor. From the extrapolation of measured $S_{\text{inc}}(\alpha,\beta)/\alpha$ for α tending to zero [i.e., $Q \to 0$ and $W(Q) \to 0$] the density of states can be easily calculated. Also, multiphonon contributions to the scattering may become important at higher temperatures, and so the data were corrected by the method described by Dianoux.[20]

The analysis outlined above was applied to the cold neutron TOF data, which were obtained using an incident wavelength of 6.5 Å. The instrumental resolution was about 100 μeV for small energy transfer, increasing rapidly with increasing energy transfer to about 7 meV at $E = 50$ meV. Spectra from different detectors were summed in order to improve the signal-to-noise ratio; taking sums over intervals $2\theta \pm 10°$ for a small and a large average value of 2θ preserves the polarization information consistent with the mosaic spread. The experiments were performed for sample temperatures $T = 280$ K, 326 K, and 473 K. In order to pass from one experimental configuration to the other, the container was simply rotated by 90°.

The FAS experiments were performed at 150 K, 200 K, and 250 K. In this technique, shown schematically in Fig. 2, monochromatic neutrons of variable energy E_i are inelastically scattered through $\sim 90°$ by the sample and detected at a fixed final energy E_f through a low-pass Bragg cutoff filter consisting of a cooled polycrystalline material (lattice constant d) which transmits only those neutrons with wavelengths longer than $2d$ (forward scattering, $\sin\theta = 1$).[21] E_f is defined by the cutoff wavelength, ~ 3 meV for beryllium and ~ 1.1 meV if powdered graphite is placed in series with the Be. We used mostly the Be-graphite combination, for which the energy resolution is of order 1–2 meV over the range of energy transfers studied. Since E_f is small compared to

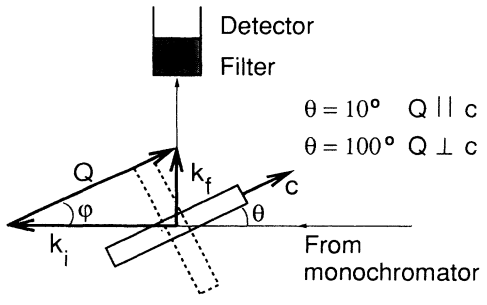

FIG. 2. Schematic configuration of the FAS technique. The polymer chain axis lies in the scattering plane. When the sample is positioned so that the incident angle $\theta = 10°$, the transfer vector $\mathbf{Q}$ is predominantly parallel to c. By rotating the sample to $\theta = 100°$ (the new position is illustrated by the dashed line) the configuration $\mathbf{Q} \perp c$ is obtained.

E_i, $\mathbf{k}_f$ is also small and the wave-vector transfer $\mathbf{Q}$ is essentially equal to, and parallel to, $\mathbf{k}_i$. This allows us to exploit the preferred orientation of the stretch-aligned polymer to obtain polarization information, as in TOF. Also, since $Q \approx k_i$, the wave-vector and energy transfers are directly coupled, and in Eq. (1) we have $\alpha/\beta \approx 1$. Thus to a good approximation the observed intensities can be directly related to the density of states. Inelastic spectra are recorded by scanning the incident energy and detecting all scattered neutrons with $E_f < E_{\text{cutoff}}$ for a fixed monitor count of incident neutrons.

Referring to Fig. 2, the filter-detector axis is at 90° to the incident beam from the monochromator. The polymer c axis lies in the scattering plane; at $\theta = 10°$ the transfer vector $\mathbf{Q}$ is mainly parallel to c, while rotating the sample to $\theta = 100°$ gives the $\mathbf{Q} \perp c$ configuration. The angle φ (between vectors $\mathbf{Q}$ and $-\mathbf{k}_i$) decreases slightly with increasing energy transfer; however, the change in φ is only $\sim 10°$ (calculated for 2-meV final neutrons) for E from 15 to 90 meV. Considering the 10° c-axis mosaicity of the polymer films, both the $\mathbf{Q} \perp c$ and $\mathbf{Q} \parallel c$ conditions were reasonably satisfied for the whole range of examined energies $15 \leq E \leq 90$ meV.

A copper Cu(220) monochromator was used for energy transfers $E > 35$ meV, while for energies below 40 meV a graphite(002) monochromator has been employed. Collimators with 40′ divergence were placed both in the pile and between the monochromator and the sample. Due to $\lambda/2$ contamination, the minimum transfer E that can be measured with this technique is limited to ~ 15 meV.

One principal difference between the TOF and FAS methods needs to be mentioned. In the cold neutron TOF we mainly detect neutrons that have absorbed the vibrational energy ($E_f > E_i$) whereas in the FAS technique we measure neutrons that have excited vibrations ($E_f < E_i$). The main consequence is a slightly different response to changes of sample temperature. At low T the peaks in FAS spectra are in general sharper and better resolved, while in TOF the vibrations at higher energies are less populated at low T, peaks are not well resolved, and long counting times are necessary. Thus it is not reasonable to study very low temperatures with the cold neutron TOF method, except at very small energy transfers. Also, the counting statistics is better with FAS than with cold neutron TOF at high-energy transfers.

III. RESULTS

Both the TOF and FAS vibrational spectra are dominated at high frequency by the intrachain dynamics. Considerable information about high-frequency intrachain modes has already been obtained from IR and Raman studies[22–24] as well as from model calculations.[25] In our experiments especially the vibrational modes involving C—H bond bending contribute strongly above 100 meV. The perpendicular component of the vibrational density of states, $G_\perp$, displays a broad band centered around 120 meV (960 cm^{-1}) as expected for out-of-plane C—H bending modes; similarly $G_\parallel$ contains a broad band above 150 meV (1200 cm^{-1}) corresponding to C—H in-

plane bending vibrations.

However, the most interesting information acquired by IINS experiments is in the low-frequency region: the lattice (interchain) modes, the phenylene ring librations, and the intramolecular torsional motions. Indeed, little is known about these modes from IR and Raman experiments. For instance in IR spectra the two lowest frequencies are resolved at 430 cm^{-1} (54 meV, ring deformation) and 558 cm^{-1} (70 meV, phenylene out-of-plane bend). Figure 3 displays the portion of TOF-derived densities of states in the 0–80 meV interval. These show several distinct features as well as obvious differences between the two polarizations. In the perpendicular polarization there are two strong distinct peaks at 15 and 25 meV, followed by a noticeable gap and a broader band with peaks at 51 meV and $\sim$ 60 meV. Most of these modes have a partially mixed character since they also appear in the parallel polarization, albeit with different proportions. A peak at 39 meV seems to be the only feature which is substantially polarized in the longitudinal direction, and only the 51 meV peak in $G_\perp$ lacks a significant counterpart in $G_\parallel$. Closer examination of the 15-meV and 25-meV features reveals that, although both are stronger in the perpendicular polarization, the 25-meV peak contributes more strongly in the parallel orientation than the one at 15 meV. Also the shapes of both 15-meV and 25-meV bands (especially in $G_\parallel$) suggest that they might actually be doublets (or even more complex structures) with $\sim$ 4-meV separation.

In general the intramolecular as well as interchain forces are not purely harmonic (otherwise the crystal would not expand on heating), which causes the frequencies of the vibrational modes to spread over a finite range. Thus with increasing temperature, as the anharmonic character of the forces increases, the peaks in the scattering spectra broaden, and also changes in the mean values of the frequencies may occur. In order to investigate such effects in PPV we carried out the IINS experiments at several temperatures.

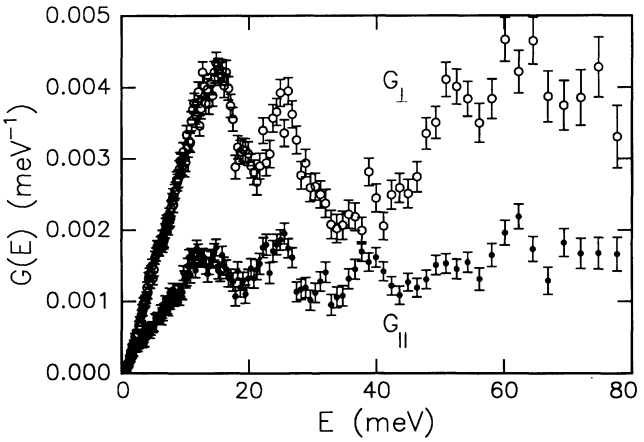

FIG. 3. Polarized vibrational density of states of PPV at 326 K. $G_\perp$ (open circles) represents the H motions polarized perpendicular to the chain axis. $G_\parallel$ (solid circles) represents motions with parallel polarization. Both $G_\perp$ and $G_\parallel$ were obtained by summing over $2\theta \pm 10°$ range of detectors for large scattering angles ($2\theta = 97°$) in the $C_\perp$ and $C_\parallel$ geometry, respectively, and normalized to unity in the range 0–200 meV.

Figure 4(a) shows the TOF-derived $G_\perp(E)$ for $T = 280$ K, 326 K, and 473 K in the 0–50 meV range; the improved statistics has been achieved by summing the response from all detectors in the $C_\perp$ geometry ($7° < 2\theta < 127°$). For comparison, $G_\parallel$ spectra at the same temperatures are depicted in Fig. 4(b); here of course only the 20° interval of detectors satisfying $\mathbf{Q} \parallel c$ in the $C_\parallel$ geometry can be summed. In the enhanced $G_\perp$ we can now resolve a $\sim$ 2-meV redshift of the 25-meV band with increasing

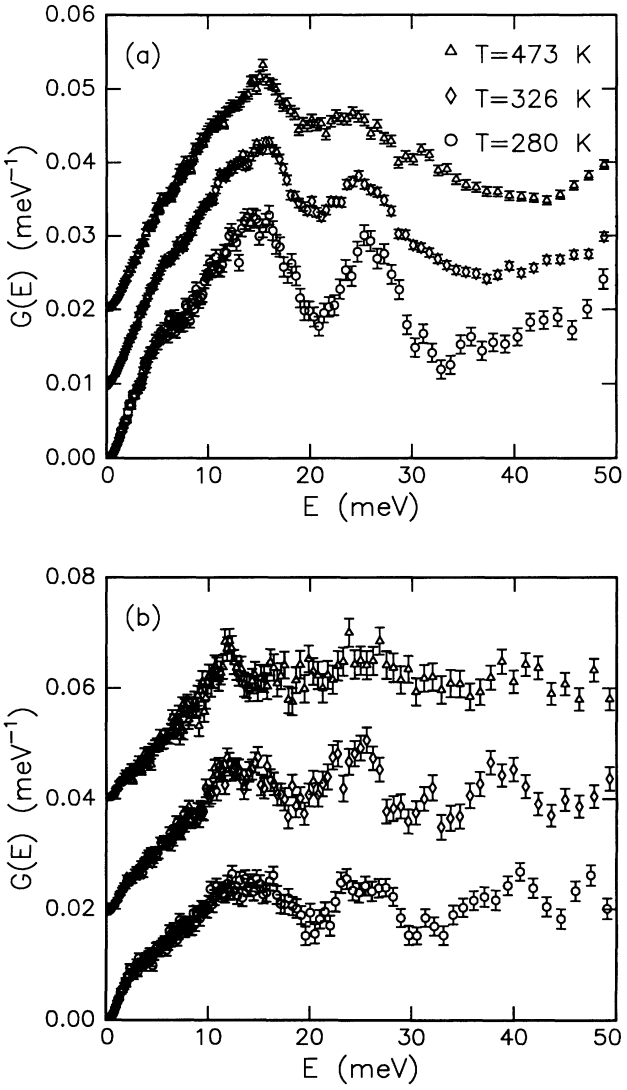

FIG. 4. (a) The effect of temperature on the perpendicular component $G_\perp$ of the density of states. The improvement of the signal-to-noise ratio was achieved in the $C_\perp$ geometry by summing the response from all detectors in $7° < 2\theta < 127°$ range. The $G_\perp(E)$'s were normalized to unity in 0–50 meV and offset vertically by 0.01 meV^{-1} for clarity. (b) The effect of temperature on $G_\parallel$. The data points (circles for $T = 280$ K, diamonds for 326 K, and triangles for 473 K) were acquired in the $C_\parallel$ geometry for $87° < 2\theta < 107°$. The $G_\parallel(E)$'s were normalized to unity in 0–50 meV and offset by 0.02 meV^{-1} for clarity.

temperature, as well as a shoulder at 7 meV which is most evident at the lowest T. This latter feature must correspond to a purely perpendicular mode because there is no trace of it in the parallel polarization. The expanded $G_{\|}$ spectra in Fig. 4(b) show the above-mentioned splitting of the first maxima as well as an abrupt change of slope, or shoulder, at 2–3 meV, again most pronounced at 280 K. This seems to be a feature with purely longitudinal polarization.

The relative contributions of phenylene rings and vinylene segments to the various features observed in $G(E)$ have been assessed by comparing FAS spectra of fully hydrogenated "H6" and 70% vinylene-deuterated "D2" samples. These are contrasted in the $\mathbf{Q} \perp c$ configuration at 150 K in Fig. 5. The two spectra are very similar; the 51-meV peak is stronger in D2 than in H6, while the weak feature near 40 meV is suppressed in D2 relative to H6. We know from the TOF results that the 40 meV feature is mainly parallel polarized, but it must also include perpendicular motion of vinylene hydrogens since it is detected somewhat more strongly in H6 than in D2. The 25-meV band appears with relatively higher intensity in H6 than in D2 which suggests that this mode also involves perpendicular motion of vinylene segments. In Fig. 6 the same 150-K D2 spectrum is contrasted with its $\mathbf{Q} \parallel c$ analog. At this temperature, all the features are remarkably well resolved. The mainly parallel character of the response near 40 meV is confirmed; in fact we can resolve two peaks at 37 and 40 meV in the parallel spectrum. A strongly parallel feature is observed near 80 meV. The peaks found with TOF at 15 meV and 25 meV are also present in both FAS polarizations, again stronger overall in perpendicular as compared to parallel, and again with the 25-meV band showing relatively more contribution in the parallel polarization than the first maximum. The response above 60 meV suggests two modes, at 61 meV with mixed polarization and at 68 meV with perpendicular polarization.

The temperature dependence of the perpendicular spectra of D2 measured with the FAS technique is shown in Fig. 7. The 51-meV intensity decreases rapidly with increasing T, and the 80-meV residuum, as well as the

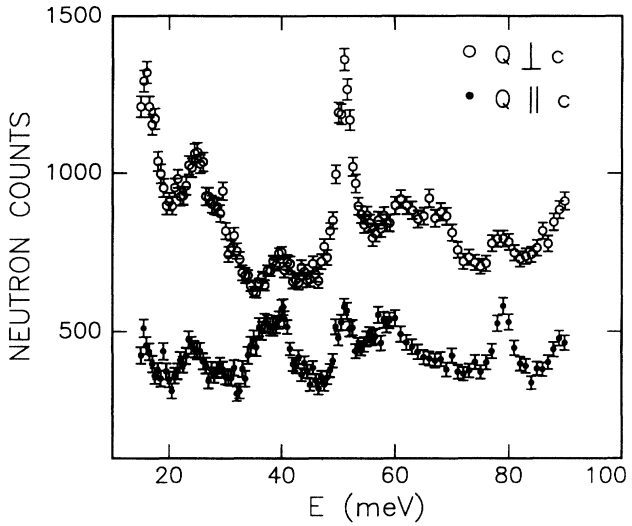

FIG. 6. The comparison of the D2-PPV spectra obtained in the parallel (solid circles) and perpendicular (open circles) configuration for sample temperature 150 K. Both spectra were measured for the same monitor count of the incident beam. The $\mathbf{Q} \perp c$ spectrum is shifted upwards by 300 counts for clarity.

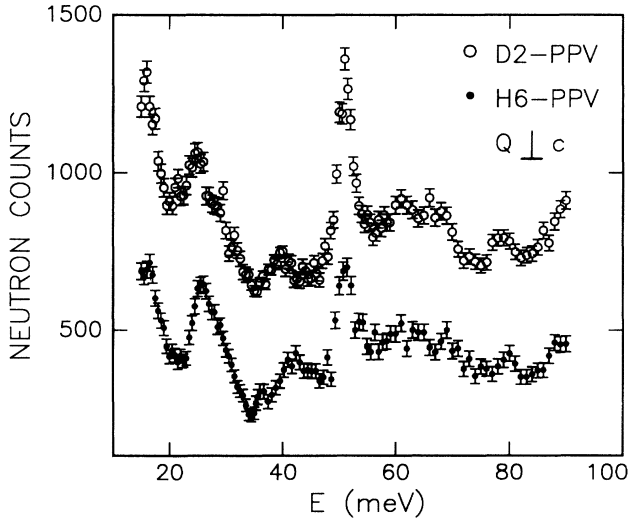

FIG. 5. The neutron-scattering spectra obtained with the filter-analyzer spectrometer in the $\mathbf{Q} \perp c$ configuration for $T = 150$ K. Solid circles correspond to the 720-mg all-hydrogen PPV sample, open circles to the 1050-mg vinylene-deuterated sample. The spectrum of the latter is shifted upwards by 300 counts for clarity. Both measurements were performed for the same monitor count of the incident beam.

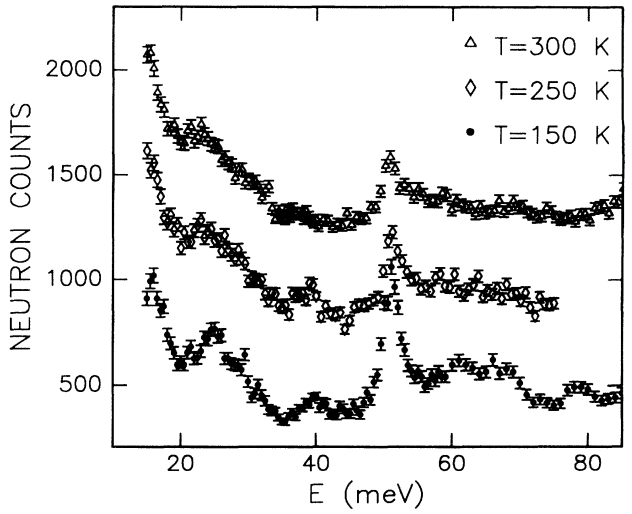

FIG. 7. Temperature dependence of the $\mathbf{Q} \perp c$ spectra of the D2-PPV sample. The negative shift of the second peak with increasing temperature is clearly visible; the same effect was observed in the all-hydrogen PPV with the TOF technique. All spectra were measured for the same monitor count of the incident beam, and are separated by 400 counts for clarity.

broader 60–70 meV feature, is completely smeared out at 300 K. Also notable is the 2-meV redshift of the 25-meV peak with increasing temperature, as was also observed in TOF spectra of H6, Fig. 4(a). The temperature dependence of this feature is therefore firmly established as an intrinsic feature of the phenylene ring dynamics.

IV. DISCUSSION

We base the assignment of peaks in IINS spectra to specific modes on polarization and isotope substitution results, IR and Raman data, analogies to the dynamics of similar polymers (mainly polyaniline and polyacetylene), and finally on our vibrational analysis of an isolated PPV chain. In the latter we used intramolecular force constants calculated by the Hartree-Fock semiempirical Austin model 1 (AM1) method[26] [compared to its parent modified neglect of differential overlap (MNDO) method, AM1 provides better molecular geometries and improved determination of torsion potentials]. An infinite polymer chain was considered (using the "cluster" method[27]) with repeating units formed by two phenylene-vinylene segments (a similar calculation yielding almost identical results was also performed for a four-segment repeat unit). Several symmetry conditions were imposed, most importantly the alternating values $+\vartheta_D$ and $-\vartheta_D$ for dihedral angles of neighboring rings. The potential energy curve which we calculate for the ring torsions is rather flat [similar results were found for *trans*-stilbene, the shortest oligomer of PPV Ref. 28]. The minimum energy molecular geometry that has been obtained has a relatively high dihedral angle $\vartheta_D = 26°$ (20° in case of the four segment repeat unit); however, the total energy of a fully coplanar chain (where $\vartheta_D = 0$ has been enforced) is only 0.33 kcal/mol C_8H_6 higher, suggesting that the packing forces in crystalline PPV may significantly reduce the dihedral angles.

It has been pointed out that by solving the vibrational secular equation for a single molecule the eigenvectors $\mathbf{e}_j^d$ for the normal modes can also be utilized to calculate the inelastic neutron scattering from an ensemble of noninteracting identical molecules.[29] The results of such a calculation for the two-segment repeat unit for $T \to 0$ are shown in Fig. 8. Here the approximation $Q^2 \sim E$ (valid for the FAS measurement) has been made, and the individual $\delta(\omega - \omega_j)$ peaks (where ω_j is the frequency of the calculated jth mode) with amplitudes given by the one-phonon emission cross section were broadened in correspondence with the FAS instrumental resolution and summed up. The polymer chains were assumed to be aligned in one direction and the scattering was calculated separately for $\mathbf{Q} \perp c$ and $\mathbf{Q} \parallel c$, assuming complete isotropy in the orientation of the molecules in the plane normal to the chain axes. The comparison of the calculated scattering with the measured spectra in the 0–100 meV range (Figs. 5 and 6) shows quite good agreement for almost all peaks with the exception of the 25-meV band, which will be discussed later.

The observed modes and their calculated counterparts are summarized in Table I. The vibrational modes found

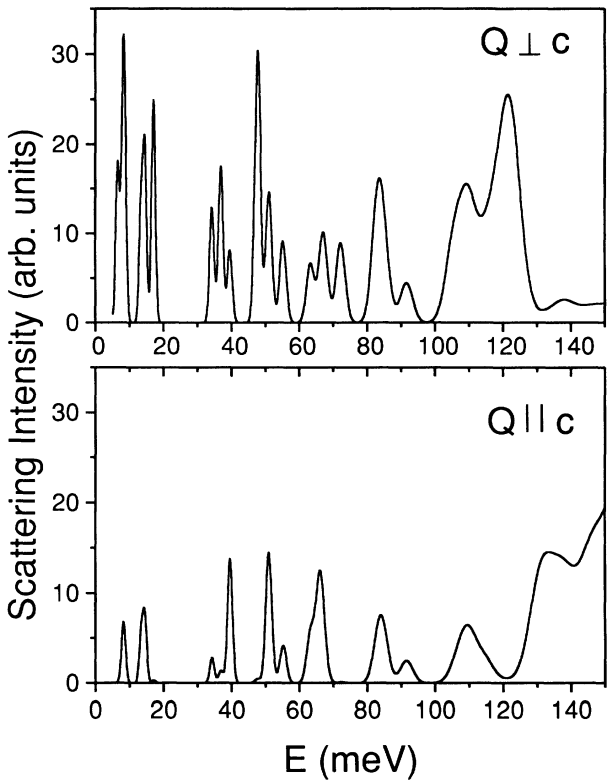

FIG. 8. Neutron-scattering spectra from PPV chains (two-segment repeat unit) based on the results of the AM1 calculation, as would be observed by the FAS instrument for $\mathbf{Q} \perp c$ (upper figure) and $\mathbf{Q} \parallel c$ (lower figure).

in the calculation that contribute most strongly in the neutron scattering are schematically depicted in Fig. 9. Rather than discuss all $3N - 4 = 80$ modes (where N is the number of atoms, $N = 28$ for two-segment repeat unit) we will focus only on the modes below 90 meV. In this frequency range the modes in question are essentially skeletal vibrations and the hydrogens are displaced with their respective C atoms to which they are connected without any considerable C—H stretching or bending. Furthermore, we found that below 40 meV the phenylene rings and vinylene groups can be considered as almost rigid units and the vibrations involve mostly rotation about and bending of the C(vinyl)—C(phenyl) bonds (this approximation has also been made in some of the diagrams in Fig. 9). Here it is necessary to mention that due to the nonplanarity of PPV, the normal modes are complex three-dimensional vibrations which are difficult to depict clearly in full detail. The diagrams in Fig. 9 were therefore slightly simplified such that the main character of the vibrations remains obvious [e.g., in Fig. 9(a) the ring librations are actually superimposed on a whole-chain oscillation in the opposite sense such that the total angular momentum is conserved].

We begin the discussion of the IINS spectra with the peaks at higher energies. The mainly parallel feature at 80 meV (640 cm^{-1}) detected by FAS (Fig. 6) is quite close to a Raman line at 661 cm^{-1} (Ref. 24) and cor-

TABLE I. Vibrational frequencies observed by IINS, AM1 calculated frequencies, polarization of the modes with respect to chain axes, and assignment of modes (i.p. = in plane, o.o.p. = out of plane).

$\hbar\omega$ [IINS] (meV)	Calc. (meV)	Polarization	Assignment
2.5	–	$\parallel c$	whole chain translations
7	8.5	$\perp c$	ring librations (in phase)
15	14.5	mixed	vinylene translations + i.p. ring librations
	17.0	$\perp c$	vinylene torsions + o.o.p. ring translations
25	25.2	$\perp c$	whole chain librations or
	(four-segment repeat unit)		mixed chain torsions and ring librations
37	–	$\parallel c$	LA mode at $q = \pi/c$
40	39.5	$\parallel c$	i.p. ring and vinylene librations
51	47.7	$\perp c$	o.o.p. ring deformations
60	63.5	mixed	i.p. ring librations (out of phase)
68	67.1	$\perp c$	o.o.p. ring deformations, out of phase,
	72.2	$\perp c$	in phase ("butterfly" mode)
80	82.6, 82.9	mixed	i.p. ring deformations (out of phase, in phase)
	84.0	mixed	i.p. ring stretching deformations

responds to longitudinal ring-stretching and in-plane deformations. Our calculations revealed modes consistent with this description at 84.1 meV and 82.6 meV (82.9 meV if the rings are deformed in phase with each other). We stress that these ring deformations do not comprise C—C bond stretching, which would place them at much higher frequencies. Also, as can be seen in Fig. 8, compared with the experiment our calculation overestimated the contribution of these modes in the perpendicular polarization.

The small perpendicular peak at 68 meV (544 cm^{-1}) which is part of the broader structure between 60 and 70 meV is not far from the IR doublet at 556 and 560 cm^{-1}.[24] This can be assigned to phenylene ring out-of-plane deformations; our AM1 calculations reveal such vibrations at 67 and 72 meV (neighboring rings being out of phase and in phase, respectively), in which the deformations can be described as phenylene ring bending about the 1,4 axis (a "butterfly" motion). In this vibration the displacement vectors are mainly perpendicular to the chain axis and hence there is no scattering for $\mathbf{Q} \parallel c$ (Fig. 6). This is also correctly reproduced by the calculation. The mixed-polarization mode near 60 meV involves significant bending of the bonds connecting phenylene and vinylene carbons, resulting in in-plane circular motion of the rings [Fig. 9(f)]. Note that since the 1,4 axes of the phenylene rings are canted with respect to the c axis, the displacements of H atoms during the in-plane circular vibration ("in-plane libration") have projections in both parallel and perpendicular directions, producing the mixed character of such modes.

At 51 meV (408 cm^{-1}) we observe a very strong, sharp peak in the FAS spectra with predominantly perpendicular polarization, Fig. 5, which is also very well resolved as a distinct feature in the TOF $G_\perp(E)$, Fig. 3. This feature is close to a very weak IR mode observed by Sakamoto *et al.*[24] at 430 cm^{-1}. On the other hand, a similarly sharp peak is found in the neutron scattering spectra of solid benzene at 412 cm^{-1},[30] where it is the lowest intramolecular vibration (out-of-plane ring bending). Our calculation reproduced such a strong perpendicular mode at 47.7 meV [Fig. 9(e)], the frequency being almost independent of the relative phases between neighboring rings. This mode corresponds in principle to the ν_{16a} vibration (in Wilson notation) of benzene (410 cm^{-1}, IR and Raman inactive) and a similar mode in *para*-disubstituted benzenes with the A_u symmetry is expected at 400 ± 20 cm^{-1}.[31] The presence of this peak also in the $\mathbf{Q} \parallel c$ spectra (Fig. 6) is probably the consequence of c-axis mosaicity (10° FWHM) which together with the dihedral angles $\vartheta_D > 0$ may result in nonzero projections of displacements in the parallel direction. We remark that our vibrational analysis has also produced a mode at 51.3 meV contributing equally in both polarizations, which involved out-of-plane ring displacements together with chain squeezing (not shown in Fig. 9). Thus it cannot be ruled out that in crystalline PPV such vibration accidentally occurs at the same frequency as the ν_{16a} mode and causes the presence of the feature at 51 meV in parallel polarization.

Figure 7 (D2-PPV, $\mathbf{Q} \perp c$) shows a rapid decrease of the scattering intensity of the 51-meV peak with increasing temperature, though the frequency of the mode remains unchanged. This drop in intensity is the consequence of the Debye-Waller factor corroborating the increase of the mean amplitude of the oscillation with T. We note that a decrease of scattering is also expected due to T induced increase of dihedrals ϑ_D (at $\vartheta_D = 0$ the vectors $\mathbf{e}_j^d$ for the ν_{16a} mode are exclusively perpendicular, but the projections $\perp c$ decrease as ϑ_D increases); unfortunately the Debye-Waller effect is much stronger and prevents such observation.

The mainly parallel-polarized 40-meV (320-cm^{-1}) mode, Fig. 3 and Fig. 6, must be associated with phenylene displacements parallel to the c axis coupled with small vinylene displacements perpendicular to the c axis. This is based on the observation that the mode in question is much stronger in H6-PPV than in D2-PPV in the $\mathbf{Q} \perp c$ configuration. Our calculations reveal a parallel mode at 39.5 meV which incorporates in-plane ring librations (in phase) supported by similar vinylene in-plane circular vibrations (in the opposite sense as the rings) and out-of-plane vinylene displacements [Fig. 9(d)]. As a result the chain is slightly stretched and squeezed, and

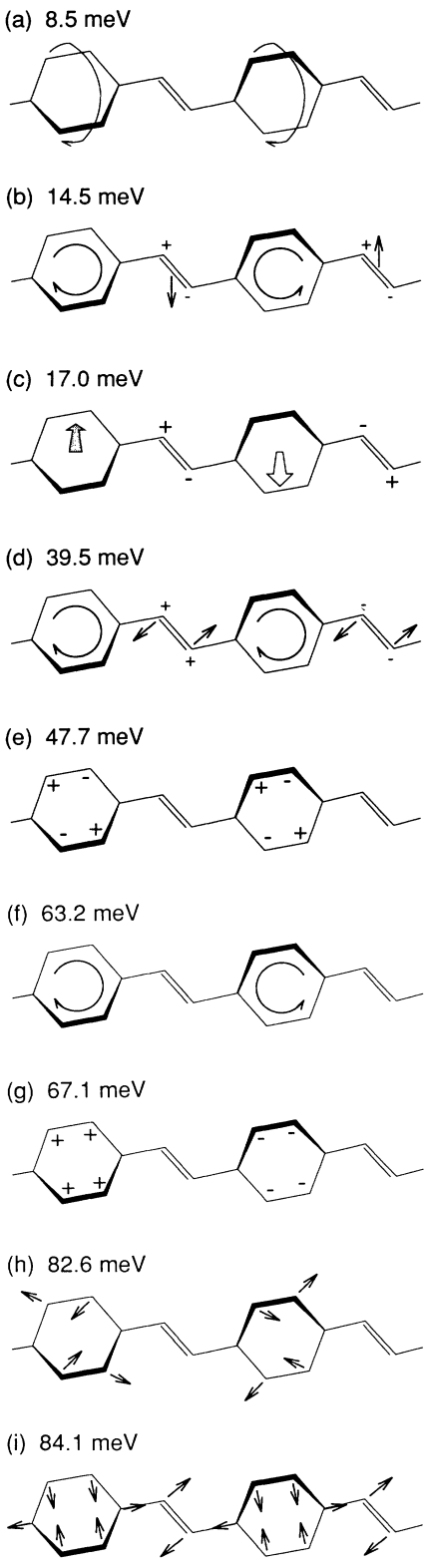

FIG. 9. Schematic representation of the calculated vibrational modes and their frequencies (see text). Simple arrows denote in-plane displacements, open and solid arrows and (+) and (−) denote out-of-plane displacements; arrows placed in the centers of phenylene or vinylene groups represent their displacements as rigid units; oblique arrows represent librations.

the scattering is stronger in the $\mathbf{Q} \parallel c$ geometry. Clearly this vibration has the character of a $q = 0$ optical phonon mode. The next parallel-polarized 37-meV (296-cm^{-1}) feature we assign to the maximum of the density of states of longitudinal acoustic modes. This contribution was generally observed in the densities of states measured from incoherent-neutron-scattering experiments. For instance, in $G(E)$ of polyacetylenes this peak was observed at 31 meV in *cis*-$(CH)_x$ (Ref. 14) and at $\sim$ 75 meV in *trans*-$(CH)_x$;[15] As can be seen in Fig. 8, in our vibrational analysis we could not identify any mainly parallel mode below 39 meV.

The precise assignment of the mainly perpendicular-polarized peaks at 15 and 25 meV is more problematic. The single-chain AM1 calculations are less reliable at lower energies, and the interchain interactions need to be taken into account. For the moment we will assume that the frequencies sustained by the lattice are close to the proper modes of a single chain and are independent of q. This is of course a very strong assumption. Deeper insight into the low-energy lattice dynamics of PPV can be achieved by more time-consuming molecular-dynamics calculations in which intramolecular *and* interchain interactions are considered. Such work is currently being undertaken.

In the perpendicular spectra we have observed three features: the weak 7-meV mode without a counterpart in $\mathbf{Q} \parallel c$, and the stronger bands at 15 and 25 meV emerging also in the parallel spectra, though with much weaker intensity. We attribute the shoulder at 7 meV in $G_\perp(E)$ [Fig. 4(a)] to purely phenylene ring librations in otherwise unperturbed chains. It appears in the frequency range in which ring librations are generally expected,[32] and peaks clearly assignable to this kind of motion were observed at 7–10 meV in polyaniline.[16] In the AM1 calculation we found such a mode at 8.5 meV [all rings librating in phase, Fig. 9(a)] and librations of individual rings (in the four-segment repeat unit calculation) were also found in the range 4.3–4.9 meV. The damped character of this mode can be understood in the view of the fact that it requires cooperative motion both of many phenylenes belonging to the same chain, and of similarly correlated phenylene motions on neighboring chains. As temperature increases, the vinylene groups are subjected to strong torsional vibrations which effectively disturb the coherency of this mode.

The strongest band at 15 meV can be attributed to the torsional motion of vinylene groups and/or transverse vinylene displacements. The calculated modes appear at 14.5 and 17 meV. The former has a more mixed character since it involves vinylene translations perpendicular to the chain axis *and* corresponding in-plane ring librations contributing also in $\mathbf{Q} \parallel c$. [Fig. 9(b)]. Contrary to the 63-meV mode [Fig. 9(f)], in this vibration the out-of-phase in-plane ring librations seem to be supported by vinylene motions. The 17-meV vibrations are out-of-plane vinylene torsions (neighboring –CH=CH– groups being out of phase) about the c axis. This type of motion translates the phenylene 1,4-axis in a direction perpendicular to the c axis, and in the vibration it is accompanied by phenylene ring out-of-plane displacements

[Fig. 9(c)], neighboring rings being out of phase. Therefore the mode can be observed also in D2-PPV, where vinylene motions do not contribute in the scattering. An analogous band in this frequency range was observed in the densities of states of *trans*- and *cis*-polyacetylene. A recent molecular-dynamics simulation of these polymers has confirmed the origin of this band as being the low-frequency internal torsional motion.[33]

An apparent disagreement between the experiment and the calculation can be seen between 20 and 30 meV. The neutron-scattering spectra (both FAS and cold neutron TOF) exhibit a broad 25-meV mainly perpendicular feature, which shifts to lower frequencies as the temperature increases. In our calculation on the two-segment repeat unit no such vibration was found. This immediately suggests that the 25-meV peak is a lattice phonon band due to interchain forces stemming most probably from whole-chain librations. Such librations (incorporating translations of phenylene as well as vinylene hydrogens) would produce stronger scattering in H6 than in D2-PPV, and indeed we have observed that the relative intensity of the second peak in Fig. 5 is higher for the all-hydrogen sample.

However, it is very interesting that a vibration close to 25 meV is obtained in the AM1 calculation when four C_8H_6 segments are considered. This vibration, calculated at 25.2 meV, has a complex character (Fig. 10) and consists of out-of-plane ring displacements, ring rocking about an axis perpendicular to the 1,4 axis, and vinylene torsions. We note that each vinylene group moves in phase with one of its neighboring vinylenes, which may be interpreted alternatively as a libration of the connecting ring. Hence, this vibration may be viewed as a combination of the 8.5- (ring libration) and 17-meV (out-of-plane ring displacement) modes [Figs. 9(a) and 9(c)] and coincidentally its frequency is also close to the sum of the frequencies of these two modes.

The frequency shift of the 25-meV band with increasing temperature seems to be directly related to the concomitant structural changes in PPV. Upon heating the PPV lattice expands[9] and the reduction of packing van der Waals forces increases the average ϑ_D. This further changes the character of interchain interactions and may quite likely cause a frequency change of whole chain librations. Alternatively, in the case of mixed vinylene torsions + ring displacements and librations the increase of ϑ_D produces significant changes of intramolecular forces and even more pronounced anharmonicity may be expected. However, until a complete lattice calculation is performed an unambiguous assignment and characterization of this band is not possible.

Both 15- and 25-meV bands are present to some extent in the parallel spectra. This nonzero parallel contribution is partially caused by the 10° c-axis mosaicity (i.e., the c axis being not perfectly parallel to the stretch direction) as well as the tilt angle between the phenylene and chain axes. Interestingly, the comparison of the $\mathbf{Q} \parallel c$ spectra with those for $\mathbf{Q} \perp c$ provides strong evidence for the complex character of these bands [see, e.g., Figs. 4(a) and 4(b)].

Finally, the lowest detected feature—the slope change of $G_{\parallel}$ at 2.5 meV [Fig. 4(b) for $T = 280$ K] is most probably associated with damped translational motion of the chains along the c axis. A similar effect was observed (and also confirmed by molecular-dynamics simulations) at 1.5 meV for *cis*-$(CH)_x$ and at 3.5 meV for *trans*-$(CH)_x$.[33,34]

V. CONCLUSIONS

With the use of incoherent inelastic neutron scattering we were able to provide important experimental insight into the lattice dynamics of poly(*p*-phenylene vinylene). By studying both all-hydrogen and vinylene-deuterated films, we have demonstrated that all of the strong vibrational features can be connected with phenylene motions. Furthermore, we have found that a strong band at 25 meV polarized mainly (but not exclusively) in the transverse direction with respect to the chain axis shows significant anharmonic character, shifting to lower frequency with increasing T (i.e., with increasing dihedral angle of the phenylene rings). To our knowledge this is the first time in the field of conducting polymers that a clear correlation between structural features and low-frequency vibrational dynamics has been established.

Our vibrational analysis based on AM1 force constants suggests possible phenylene ring librations near 25 meV coupled with considerable chain torsions and "wobble" of the ring axis. An alternative explanation is to assign this band to whole chain librations; e.g., in crystalline *trans*-polyacetylene this type of motion has been identified[34] (assuming rigid chains) at 20 meV in agreement with experiment. In fact it is possible that these two modes have very similar frequencies so that we cannot separate them in our experiments. Then, due to the proximity of the wobbling librations and whole-chain oscillations, simple resonance phenomena may cause considerable librational

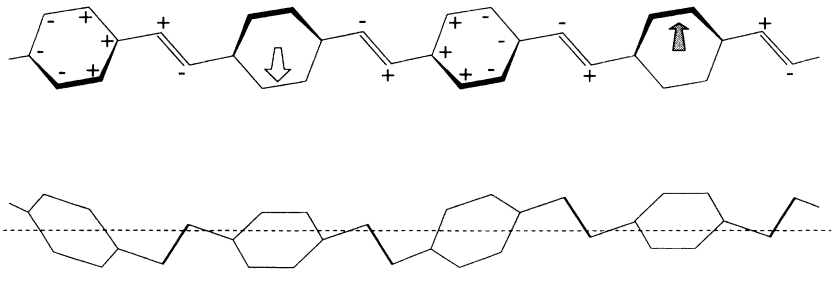

FIG. 10. Calculated vibrational mode at 25.2 meV in the four-segment repeat unit AM1 calculation. Upper figure, side view of the chain; lower figure, top view (the dashed line denotes the equilibrium vinylene plane). The displacements are exaggerated for clarity.

amplitudes. Such an effect might explain the six orders of magnitude increase of ring flips over a 200-K temperature interval observed by Simpson *et al.*[10]

A weak 7-meV feature in the perpendicular component of $G(E)$ was attributed to coherent in-phase libration of phenylene groups. If this is correct, the neutron-scattering technique may be an interesting tool for determining the nature of PPV chains after doping. For instance, n doping (as in Na-doped PPV) adds electrons to the chain and a radical anion extending over several repeat units is formed. As a result, the bond order of the C(phenyl)—C(vinyl) bond increases, which should also affect the energy of phenylene librations. However, doping also induces a rearrangement of the lattice of polymer chains, which may complicate the assignment of phonon frequencies. On the other hand, the change of electronic structure should also have an effect on the out-of-plane phenyl ring deformations (51 and 68 meV in pristine PPV) which are readily observed by IINS. The neutron-scattering study of Na-doped PPV is currently in progress.

ACKNOWLEDGMENTS

This work was supported by the National Science Foundation MRL Program under Grant No. DMR91-20668. We would like to thank D. A. Neumann, J. J. Rush, and T. Udovic for helpful discussions and technical assistance, and one of us (J.E.F.) is particularly grateful to the entire staff of the Reactor Radiation Division at NIST for their hospitality during a sabbatical leave. The technical assistance of G. Coddens and R. Kahn of the Laboratoire Léon Brillouin (CEN, Saclay, France) is also gratefully acknowledged.

[1] J. H. Burroughes, D. D. C. Bradley, A. R. Brown, R. N. Marks, K. Mackay, R. H. Friend, P. L. Burn, and A. B. Holmes, Nature **347**, 539 (1990).
[2] T. Kaino, K. Kubodera, S. Tomaru, T. Kurihara, S. Saito, T. Tsutsui, and S. Tokito, Electron. Lett. **23**, 1095 (1987).
[3] M. Hirooka, I. Murase, T. Ohnishi, and T. Naguchi, in *Frontiers of Macromolecular Science*, edited by T. Saegusa (Blackwell Scientific, Oxford, 1989), p. 425.
[4] C. Zhang, D. Braun, and A. J. Heeger, J. Appl. Phys. **73**, 5177 (1993).
[5] D. R. Gagnon, F. E. Karasz, E. L. Thomas, and R. W. Lenz, Synth. Met. **20**, 85 (1987).
[6] D. D. C. Bradley, R. H. Friend, T. Hartmann, E. A. Marseglia, M. M. Sokolowski, and P. D. Townsend, Synth. Met. **17**, 473 (1987).
[7] T. Granier, E. L. Thomas, D. R. Gagnon, R. W. Lenz, and F. E. Karasz, J. Polym. Sci., Polym. Phys. Ed. **24**, 2793 (1986).
[8] T. Granier, E. L. Thomas, and F. E. Karasz, J. Polym. Sci., Polym. Phys. Ed. **26**, 65 (1988).
[9] D. Chen, M. J. Winokur, M. A. Masse, and F. E. Karasz, Polymer **33**, 3116 (1992).
[10] J. H. Simpson, D. M. Rice, and F. E. Karasz, J. Polym. Sci., Polym. Phys. Ed. **30**, 11 (1992).
[11] G. Mao, J. E. Fischer, F. E. Karasz, and M. J. Winokur, J. Chem. Phys. **98**, 712 (1993).
[12] P. A. Heiney, J. E. Fischer, D. Djurado, J. Ma, D. Chen, M. J. Winokur, N. Coustel, P. Bernier, and F. E. Karasz, Phys. Rev. B **42**, 2507 (1991).
[13] H. S. Woo, O. Lhost, S. C. Graham, D. D. C. Bradley, R. H. Friend, C. Quattrocchi, J. L. Brédas, R. Schenk, and K. Müllen, Synth. Met. **59**, 13 (1993).
[14] J. L. Sauvajol, D. Djurado, A. J. Dianoux, N. Theophilou, and J. E. Fischer, Phys. Rev. B **43**, 14305 (1991).
[15] J. L. Sauvajol, D. Djurado, A. J. Dianoux, and J. E. Fischer, J. Chim. Phys. (Paris) **89**, 969 (1992).
[16] J. L. Sauvajol, D. Djurado, A. J. Dianoux, J. E. Fischer, E. M. Scherr, and A. G. MacDiarmid, Phys. Rev. B **47**, 4959 (1993).
[17] D. R. Gagnon, J. D. Capistran, F. E. Karasz, R. W. Lenz, and S. Antoun, Polymer **28**, 567 (1987).
[18] J. M. Machado, F. E. Karasz, R. V. Kovar, J. M. Burnett, and M. A. Druy, New Polym. Mater. **1**, 189 (1989).
[19] M. Bée, *Quasielastic Neutron Scattering* (Adam Hilger IOP, London, 1988), p. 63.
[20] A. J. Dianoux, Philos. Mag. B **59**, 17 (1989).
[21] R. R. Cavanagh, J. J. Rush, and R. D. Kelley, in *Vibrational Spectroscopy of Molecules on Surfaces*, edited by J. T. Yates and T. E. Madey (Plenum, New York, 1987), p. 183.
[22] S. Lefrant, E. Perrin, J. P. Buisson, H. Eckhard, and C. C. Han, Synth. Met. **29**, E91 (1989).
[23] B. Tian, G. Zerbi, and K. Müllen, J. Chem. Phys. **95**, 3198 (1991).
[24] A. Sakamoto, Y. Furakawa, and M. Tasumi, J. Phys. Chem. **96**, 1490 (1992).
[25] D. Rakovic, R. Kostic, I. E. Davidova, and L. A. Gribov, Synth. Met. **55**, 541 (1993).
[26] M. J. S. Dewar, E. G. Zoebish, E. F. Healy, and J. J. P. Stewart, J. Am. Chem. Soc. **107**, 3902 (1985).
[27] J. J. P. Stewart, New Polym. Mater. **1**, 53 (1987).
[28] O. Lhost and J. L. Brédas, J. Chem. Phys. **96**, 5279 (1992).
[29] D. A. Neumann (private communication).
[30] J. H. Williams, Chem. Phys. **167**, 215 (1992).
[31] See, e.g., F. R. Dollish, W. G. Fateley, and F. F. Bentley, *Characteristic Raman Frequencies of Organic Compounds* (J. Wiley, New York, 1974), p. 162, and references therein.
[32] J. M. Ginder and A. J. Epstein, Phys. Rev. B **41**, 10674 (1990).
[33] A. J. Dianoux, G. R. Kneller, J. L. Sauvajol, and J. C. Smith, J. Chem. Phys. **99**, 5586 (1993).
[34] P. Papanek and J. E. Fischer, Phys. Rev. B **48**, 12566 (1993).

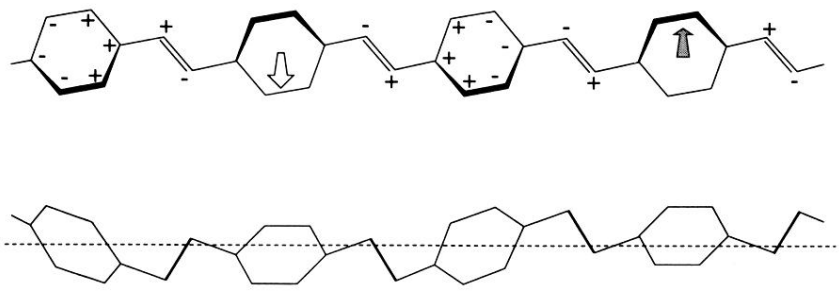

FIG. 10. Calculated vibrational mode at 25.2 meV in the four-segment repeat unit AM1 calculation. Upper figure, side view of the chain; lower figure, top view (the dashed line denotes the equilibrium vinylene plane). The displacements are exaggerated for clarity.

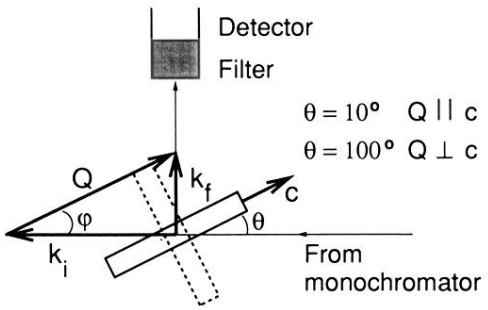

FIG. 2. Schematic configuration of the FAS technique. The polymer chain axis lies in the scattering plane. When the sample is positioned so that the incident angle $\theta = 10°$, the transfer vector $\mathbf{Q}$ is predominantly parallel to c. By rotating the sample to $\theta = 100°$ (the new position is illustrated by the dashed line) the configuration $\mathbf{Q} \perp c$ is obtained.

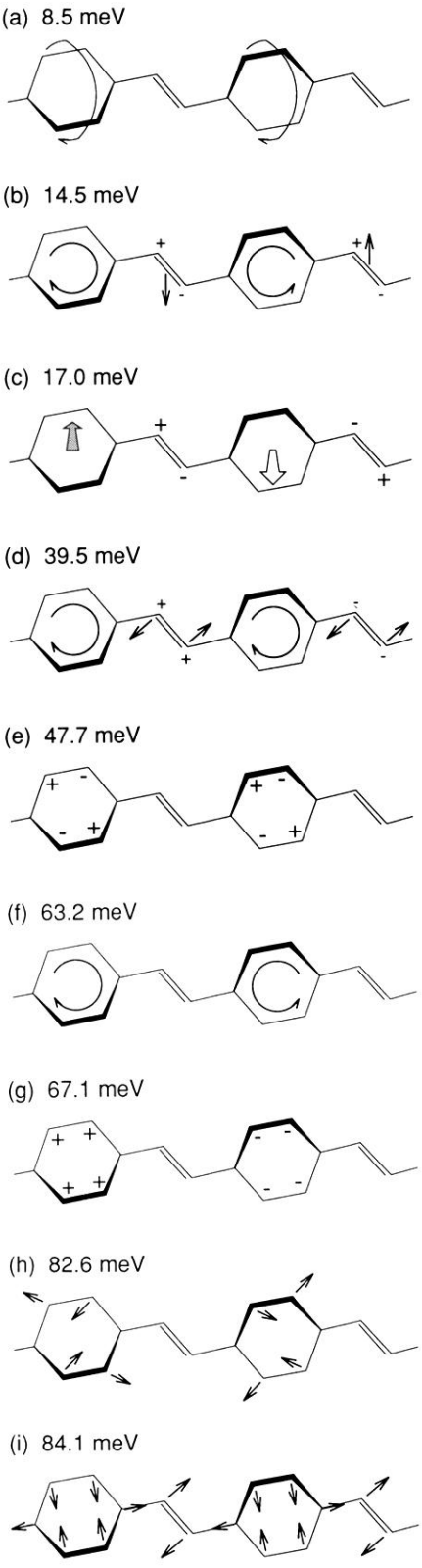

FIG. 9. Schematic representation of the calculated vibrational modes and their frequencies (see text). Simple arrows denote in-plane displacements, open and solid arrows and (+) and (−) denote out-of-plane displacements; arrows placed in the centers of phenylene or vinylene groups represent their displacements as rigid units; oblique arrows represent librations.